Sustainable Materials and Technologies 5 (2015) 1–8

Contents lists available at ScienceDirect

Sustainable Materials and Technologies

Sustainable injection moulding: The impact of materials selection and gate location on part warpage and injection pressure

Marton Huszar *, Fawzi Belblidia, Helen M. Davies, Cris Arnold, David Bould, Johann Sienz

College of Engineering, Swansea University, Singleton Park, Swansea SA2 8PP, UK

ARTICLE INFO

Article history:
Received 18 May 2015
Received in revised form 3 July 2015
Accepted 11 July 2015
Available online 20 July 2015

Keywords:
Gate location
Injection moulding
Injection pressure
Part warpage

ABSTRACT

This paper presents an approach of how warpage (i.e. part deflection) and injection pressure of an intricate geometry could be minimised by selecting an optimal thermoplastic material and injection gate location (through which the molten plastic flows into the cavity). The numerical analyses for mould filling considered four gate locations along with a PP (polypropylene), PS (polystyrene) and a fibre-filled PP material (each had different shrinkage characteristics, mechanical property and viscosity). Results of the cavity filling simulations indicated that (on average) the largest and smallest warpage was predicted with the PP and PS respectively. The warpage of the fibre-filled PP showed the most gate location dependent behaviour. In addition, the lowest injection pressure was associated with the fibre-filled PP. For reduced pressure, the best and second best solutions for gate location were the top and middle ones. In addition, specific attention was paid to differential fibre orientation, as one of the most important factors responsible for part warpage. In an attempt to maximise the part stiffness, the fibre-filled PP was selected. It became clear that the gate location affected the melt flow evolution and therefore the fibre orientation. Simulation results showed that bidirectional flow and asymmetrical fibre distribution was achieved with the gate positioned at the mid-section of the part. Unidirectional flow and therefore symmetrical fibre distribution could be achieved by placing the gate at the top section of the part. The injection moulding experimental utilised the fibre-filled PP along with the two aforementioned gate locations. It was discovered that warpage was present when the middle gate was applied, but it was successfully eliminated using the top gate location. It can be stated that differential fibre orientation did not cause warpage, but the asymmetrical distribution of fibre orientation did. The information discussed in the paper may be particularly useful in the early mould/part design stages when any modification can still be easily and cost-effectively implemented. An important finding is that the final gate location should only be chosen after the thermoplastic material properties and melt flow direction have been taken into account. The successful reduction of warpage and injection pressure may help to reduce the amount of production waste and energy consumption, ensuring defect-free sustainable manufacturing.

1. Introduction and literature review

Thermoplastics injection moulding is regarded as one of the most important processes that can be used to produce plastic products [1]. It commences with feeding solid plastic material (usually granules) through the hopper to the heated injection barrel. In the plastication stage, the injection screw rotates and transports molten material to the screw chamber in front of the screw tip. When sufficient amount of molten material is prepared, the plastication stops [2].

During the filling stage, the part to be formed is achieved by injecting molten material into a mould cavity. The location of the injection gate is of great importance since it can influence the flow direction and melt solidification during and after filling [3]. When the cavity is nearly filled, the injection stage is followed by the packing stage, during which period additional pressure is applied to force more molten material into the cavity to compensate for material shrinkage [4]. Then, the cooling stage removes the remaining heat from the melt with the aid of cooling channels positioned inside the mould. The process ends with the opening of the mould half (or halves) and the solidified parts are removed by the means of ejector pins [5]. In Fig. 1 a schematic is presented, describing the steps involved in the moulding process.

This cyclic process has widely been regarded as a quick and efficient technology where the production of complex geometries with intricate features is achievable. The whole process is controlled by numerous physical parameters and it is recognised that there is correlation among the process parameters, materials, part geometry and the quality of the moulded parts [6].

In one study cavity balancing was emphasised as being an important criterion during filling analyses to improve the quality of the moulded

* Corresponding author.
E-mail address: m.huszar@swansea.ac.uk (M. Huszar).

http://dx.doi.org/10.1016/j.susmat.2015.07.001

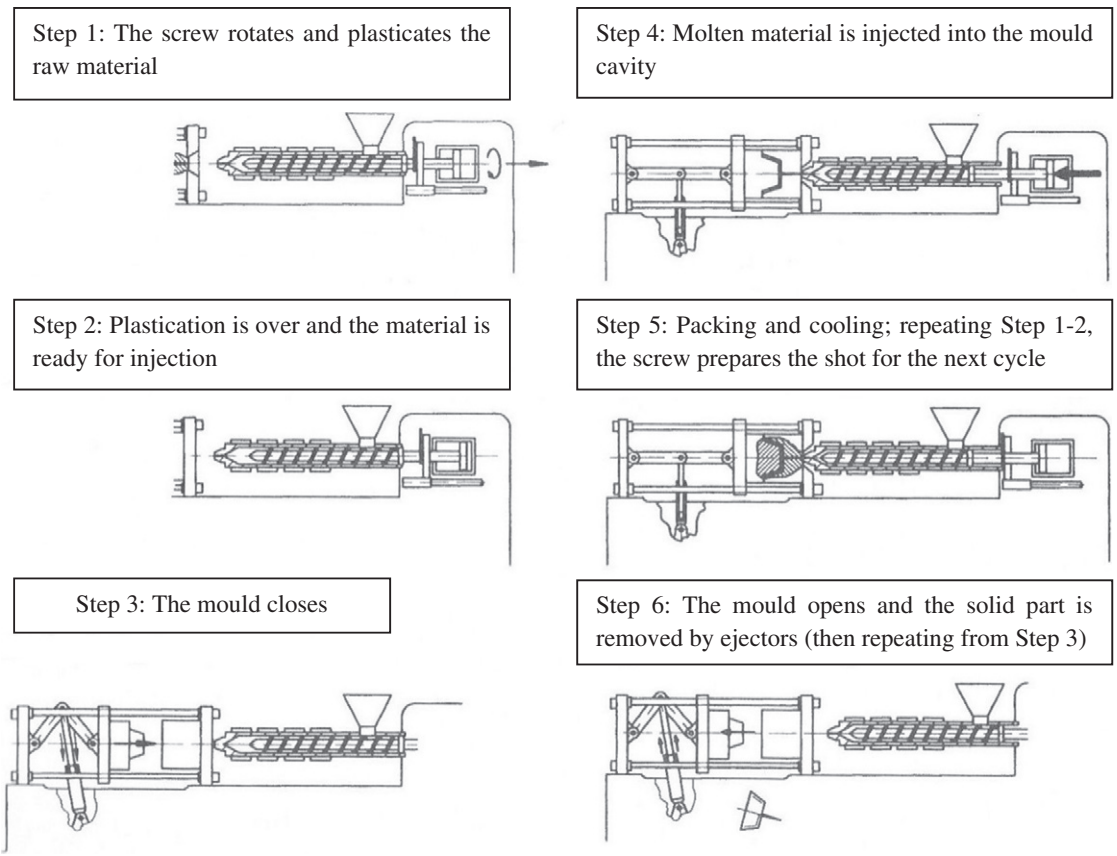

Fig. 1. The representation of the complete injection moulding cycle [2].

parts. If an unbalanced flow pattern existed, that would lead to (over-)packing difficulties and part warpage [7]. Also, the appropriate selection of gate position would help to reduce the filling time and balance the moulded parts' temperature distribution [8]. The incorrect selection of process conditions may result in undesirable shrinkage, warpage [9], unbalanced fill or deterioration of mechanical or optical properties [10].

Among the aforementioned moulding problems, the present paper focuses on part warpage and injection pressure. Prior to discussing warpage, it is necessary to describe the principle difference of shrinkage characteristics of thermoplastic materials. The Pressure–Volume–Temperature (PVT) diagrams provide information with respect to change in specific volume as a function of melt processing temperature and pressure applied on the melt. For amorphous and crystalline materials the specific volume in the melt range varies linearly with the temperature. When pressure is applied on the melt, the specific volume decreases, hence its reciprocal value, the density increases. Upon reaching the transition temperature below which the material is considered solid, amorphous and crystalline materials differ in shrinkage characteristics. Amorphous materials exhibit a linear variation, while crystalline grades show an exponential dependence of specific volume on temperature just below the transition temperature. Owing to the fact the crystalline grades consist of crystalline and amorphous phases, the crystallization phenomenon during solidification causes an orderly, consequently more densely packed microstructure. The formation of the crystalline phase results in greater density and therefore greater shrinkage, compared to amorphous grades [2].

It should be pointed out that uniform shrinkage will not cause warpage, however the variation in shrinkage will [9]. For warpage, the following major factors or the combination of these can contribute towards this quality problem.

Differential shrinkage can be caused by variations in part wall thickness. Upon solidification the larger thickness undergoes higher shrinkage. If the part is ejected before thicker region has cooled, there will be an increased variation in shrinkage between thick and thin regions [9]. In direct relation to this, variation in melt cooling rates (deviations in part temperature distribution) can cause variation in crystalline content increasing the likelihood of warpage.

Moulding process conditions may also induce variations in shrinkage. To control the formation of frozen layer and warpage, the appropriate selection of injection time, melt temperature [11], packing pressure [12] and packing time would be necessary [13]. Not only have the processing conditions played an important role in reduction of warpage but also part design as well. The warpage might be improved by introducing ribs which were to enhance the part's structural integrity [14]. Moreover, selecting a material that has low stiffness may cause greater warpage as it will have less resistance to distortion, while greater stiffness may help to improve the overall warpage [9]. For fibre-filled materials, greater warpage might be expected to occur with increased fibre volume fraction [15].

Also, differential mould cooling conditions can cause temperature deviation between the mould core and cavity surfaces. The melt suffers greater shrinkage at higher temperature areas, while lower shrinkage is observed at areas where the temperature is lower [16]. Here, the bending moment created by thermally-induced residual stress will cause the part to warp towards the hotter areas [9]. To override this problem the careful selection of cooling time and/or melt temperature would be necessary [17]. Further difficulties may arise if injection moulding is coupled with the in-mould roller (surface decoration) technique. For that, the thermal (e.g. heat retardation) effect of the film can also be a critical parameter than can affect the mould temperature distribution and final part warpage [18].

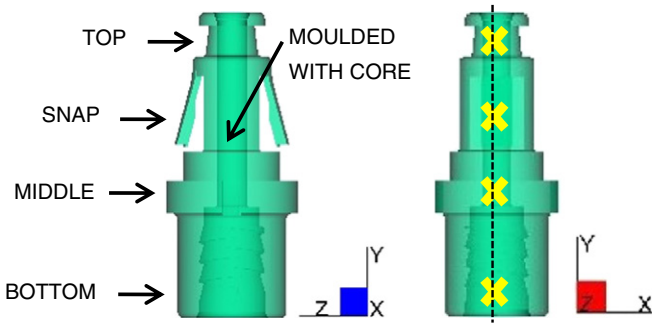

Fig. 2. The geometry under consideration.

Moreover, differential molecular orientation may cause variations in shrinkage. In a shear driven flow, a higher level of shrinkage may be observed parallel to the flow direction compared to perpendicular to the flow direction. However, for fibre-filled materials the orientation of the fibres has more effect than the molecular orientation [9]. During solidification the parallel orientation of fibres relative to the flow direction would represent unrestricted shrinkage whilst restricted shrinkage would occur if fibres are aligned perpendicular to flow direction [19]. Thus, the thermal shrinkage parallel to the main fibre orientation direction is approximately the half of that perpendicular to the main fibre orientation [20]. As a result, a bending moment due to differential fibre orientation is generated. The part will warp towards areas where unrestricted shrinkage exists.

Since parts in reality do not always have uniform thickness, hence variation in cooling rate, fibre orientation may occur during processing. The end result will be a complex distribution of variable shrinkage from region to region of the part, resulting in part warpage [5].

Besides part warpage, the injection pressure also has of importance during manufacturing, since it may determine the moulding window (i.e. the moulding process boundaries) of the parts. If insufficient injection pressure is available the cavity filling and packing might not be possible under specific process conditions, causing undesirable delay or interruption of production.

2. Materials and methods

The aforementioned review revealed that there has been a complex relationship among moulding conditions, part design and quality. To summarise these findings, it is therefore critical to take into account not only the mechanical properties of the thermoplastic material, but the melt flow direction and any change in fibre orientation in order to reduce the warpage.

To gain further knowledge how the quality of a part could be improved, it is desirable to extend the existing research with the present case study which will be explained here.

There may be a research gap regarding a systematic investigation of the combined effects of material selection and gate location. The work was carried out in an attempt to minimise the warpage and injection pressure taking into account some of the key thermoplastic material properties (e.g. elastic and shear moduli, linear thermal expansion and viscosity).

This paper departs from the utilisation of different statistical experimental techniques but aims to present a methodology through which the improvement of warpage and reduction of injection pressure may be realised.

Part warpage can be a critical concern for several engineering applications. For instance, plastic covers and housings can be joined together to form more complex assemblies. Even the smallest part misalignment may cause incomplete/loose fitness or compromise the load-bearing capacity, resulting in premature component failure. Therefore the elimination of this problem is crucial in order to produce defect-free high quality products. In addition, the injection pressure may determine the moulding window (i.e. the moulding process boundaries) of the parts. For instance, if insufficient injection pressure is available the cavity filling and packing might not be possible under specific process conditions, causing undesirable delay or interruption of manufacturing. Since any modification or replacement of existing moulds may be too costly, therefore the utilisation of simulation tools prior to real production can be used effectively to determine the injection moulding feasibility of prospective designs.

With the careful selection of thermoplastic material and gate location, minimised injection pressure could be achieved which may help to extend the moulding window, allowing a wider range of process conditions set during the moulding process. As a direct benefit, it may help to reduce energy consumption and manufacturing waste. Such questions related to sustainable manufacturing have been increasingly considered as strategic objectives within engineering companies [21].

Problems associated with improper gate location, warpage, injection pressure and other issues can all be addressed at the early design stage, resulting in both shorter overall development time and improved part quality [22].

The computational work utilised Moldflow Insight's "Fill + Pack + Warpage" analysis sequence to investigate the moulding characteristics of a partially symmetrical, hollow geometry using four potential gate locations that are illustrated in Fig. 2. The total length of the part was 48 mm and the maximum width was 20 mm respectively. The top-, snap-, middle and bottom gates were positioned 4, 19, 30, and 43 mm far from the top of the part along the YZ parting plane, respectively.

The numerical analyses were based on the 3D Navier–Stokes flow solver with governing Eqs. (1)–(5) [23] for mass, momentum and energy respectively:

$$\text{Mass}: \frac{\partial \rho}{\partial t} + \frac{\partial(\rho u)}{\partial x} + \frac{\partial(\rho v)}{\partial y} + \frac{\partial(\rho w)}{\partial z} = 0 \tag{1}$$

$$\text{Momentum}: \rho\left(\frac{\partial u}{\partial t} + u\frac{\partial u}{\partial x} + v\frac{\partial u}{\partial y} + w\frac{\partial u}{\partial z}\right) = -\frac{\partial p}{\partial x} + \eta\left(\frac{\partial^2 u}{\partial x^2} + \frac{\partial^2 u}{\partial y^2} + \frac{\partial^2 u}{\partial z^2}\right) + \rho g_x \tag{2}$$

Table 1
Material properties of the thermoplastic grades [26].

Properties		Mechanical				Flow
Grade type	Microstructure	Elastic modulus, E [MPa]	Shear modulus, G [MPa]	Linear thermal expansion, α [$\cdot 10^{-5}$/°C]	Poisson ratio[b], ν [−]	Viscosity[c], η_0 [Pa·s] (at temp. [°C])
PP	Crystalline, unfilled	~1340	~480	~9.1	~0.39	~2230 (236)
PS	Amorphous, unfilled	~1900	~690	~8.4	~0.38	~1650 (230)
PP 30%	Crystalline, 30% fibre-filled	~5050 (1st)[a] ~2700 (2nd)[a]	~1200	~2.6 (1st)[a] ~6.4 (2nd)[a]	~0.43 ~0.46	~100 (240)

[a] 1st and 2nd indicate values of parallel and normal to flow orientation.
[b] ν may be derived from E and G.
[c] Approximated zero-shear rate viscosity at 1 1/s shear-rate.

$$\rho\left(\frac{\partial v}{\partial t}+u\frac{\partial v}{\partial x}+v\frac{\partial v}{\partial y}+w\frac{\partial v}{\partial z}\right)=-\frac{\partial p}{\partial y}+\eta\left(\frac{\partial^2 v}{\partial x^2}+\frac{\partial^2 v}{\partial y^2}+\frac{\partial^2 v}{\partial z^2}\right)+\rho g_y \quad (3)$$

$$\rho\left(\frac{\partial w}{\partial t}+u\frac{\partial w}{\partial x}+v\frac{\partial w}{\partial y}+w\frac{\partial w}{\partial z}\right)=-\frac{\partial p}{\partial z}+\eta\left(\frac{\partial^2 w}{\partial x^2}+\frac{\partial^2 w}{\partial y^2}+\frac{\partial^2 w}{\partial z^2}\right)+\rho g_z \quad (4)$$

$$\text{Energy}: \rho C_p\left(\frac{\partial T}{\partial t}+u\frac{\partial T}{\partial x}+v\frac{\partial T}{\partial y}+w\frac{\partial T}{\partial z}\right)=k\left(\frac{\partial^2 T}{\partial x^2}+\frac{\partial^2 T}{\partial y^2}+\frac{\partial^2 T}{\partial z^2}\right)+\eta\gamma^2 \quad (5)$$

where ρ is the density, u, v and w are velocity vectors, x, y and z are Cartesian coordinates, p is the pressure, t is the time, g is the gravitational force, T is the temperature, C_p is the heat capacity and k is the thermal conductivity and γ is the shear-rate respectively. As defined by Eq. (6), the tracking of the melt flow front was implemented by the level set method (LSM) [5] (which is an alternative to the volume of fluid (VOF) technique):

$$\frac{\partial \varphi}{\partial t}+u\frac{\partial \varphi}{\partial x}+v\frac{\partial \varphi}{\partial y}+w\frac{\partial \varphi}{\partial z}=0 \quad (6)$$

where the φ level set function defines the distance to the melt flow front anywhere in the computational domain ($\varphi=0$ is the position of the melt/air interface, while $\varphi<0$ and $\varphi>0$ refer to any point within the melt and air, respectively). Also, as set out by Eqs. (7)–(8) [5] the η viscosity of melt based was based on the Cross-WLF model:

$$\eta=\frac{\eta_0}{1+\left(\frac{\eta_0\gamma}{\tau^*}\right)^{1-n}} \quad (7)$$

$$\eta_0=D_1\exp\left(\frac{-A_1(T-T_g)}{A_2+(T-T_g)}\right) \quad (8)$$

where η_0 is the zero-shear rate viscosity, τ^*, n, D_1, A_1, A_2 and T_g are material constants. Furthermore, as set out by Eq. (9) [24], the overall non-isothermal heat transfer during numerical analyses was calculated by the transient 3D Poisson equation:

$$\rho c_p\frac{\partial T}{\partial t}=k\left(\frac{\partial^2 T}{\partial x^2}+\frac{\partial^2 T}{\partial y^2}+\frac{\partial^2 T}{\partial z^2}\right). \quad (9)$$

The stress is described by the force balance equation, set out by Eq. (10):

$$\nabla\cdot\sigma=0 \quad (10)$$

where σ is the Cauchy stress tensor. Eqs. (1)–(5) and (7)–(9) were coupled to solve for 3D pressure, temperature and velocity components at each node [9] using the algebraic multigrid (AMG) computational technique. Then, by utilising Eqs. (9)–(10), a heat transfer and stress analysis (with body forces neglected) were solved to simulate the part warpage [5]. The computation considered the following initial and boundary conditions, as defined by Eqs. (11)–(15) [4,5,23,25]:

$$\text{At mould wall}: u,v,w=0; T=T_{wall} \quad (11)$$

$$\text{At mould wall in normal direction}: \frac{\partial p}{\partial n}=0 \quad (12)$$

$$\text{At part centre-line}: \frac{\partial u}{\partial z}=\frac{\partial v}{\partial z}=\frac{\partial w}{\partial z}=\frac{\partial T}{\partial z}=0 \quad (13)$$

$$\text{At inlet}: p_{inlet}=p(x,y,z,t);\quad T_{inlet}=T_{melt}; \phi_{inlet}<0 \quad (14)$$

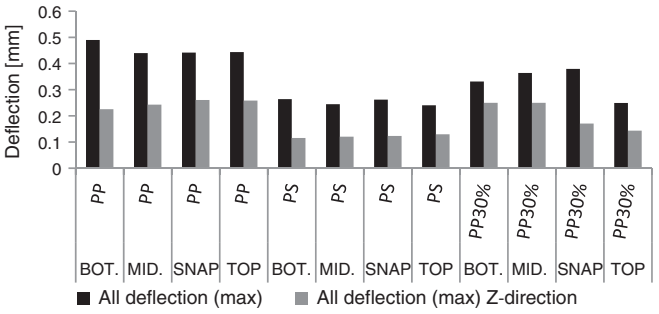

Fig. 3. Part deflection predicted by numerical analysis.

$$\text{At flow front}: p=0. \quad (15)$$

In regard to material selection, some of the relevant properties of the grades are presented in Table 1 (due to length constraints the PVT data is not listed within, but reference to this was made in Section 1). Both the gate locations and materials were chosen to ensure a good comparison into the warpage and flow characteristics of each design alternative.

To assess the part's resistance against deformation the following mechanical properties (i.e. tensile and shear moduli, thermal expansion and Poisson ratio [5]) were essential for the warpage structural analysis. Concerning the flow characteristics, the (zero shear-rate) viscosity (it's temperature dependency is characterised by Eqs. (7)–(8) was chosen as a reference parameter which may be regarded as one of the most important properties influencing the injection pressure requirement.

For each analysis the following initial (process) conditions were set: $T_{melt}=240$ °C melt temperature, 1 s injection time with packing pressure set to 80% of the filling pressure maintained for 5 s. For the mould, a $T_{wall}=40$ °C steady-state mould wall temperature boundary condition was applied, ensuring that warpage due to differential mould cooling effects could be eliminated. In addition, to ensure the parts were completely solidified, the duration of cooling period was defined on the basis of part ejection criteria (40 °C mould temp., 80, 90, and 95 °C ejection temp. For the PP, PS, and PP 30% fibre-filled respectively and 100% frozen volume).

For the PP 30% fibre-filled grade a fibre orientation analysis was also performed based on Moldflow's Folgar–Tucker model, in accordance with Eq. (16) [5]:

$$\frac{Da_{ij}}{Dt}=W_{ik}a_{kj}-a_{ik}W_{kj}+\frac{a_r^2-1}{a_r^2+1}\left(D_{ik}a_{kj}+D_{jk}a_{ki}-2D_{kl}a_{ijkl}\right)+2C_I\gamma(\delta_{ij}-3a_{ij}) \quad (16)$$

where a_{ij} and a_{ijkl} are second and forth order tensors, W is the vorticity tensor, a_r is the fibre aspect ratio, C_I is the fibre interaction coefficient [27] and δ is the unit tensor respectively. The analysis returns

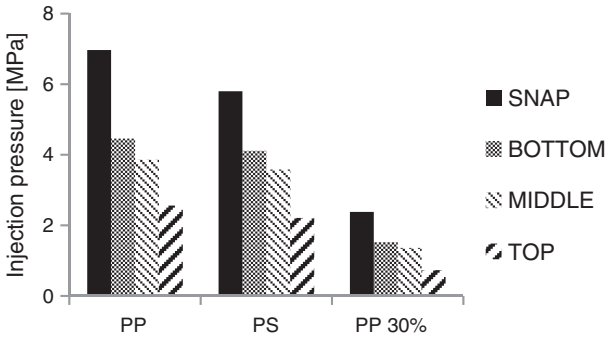

Fig. 4. Injection pressure at the end of cavity filling.

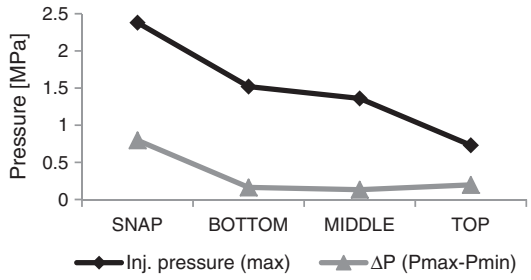

Fig. 5. Injection pressure and pressure loss for the PP 30% fibre-filled grade.

the fibre orientation tensor contour plot, which can be interpreted as the probability of orientation from region to region of the part (on contour plot result high probability is 1 and low is 0 respectively) [26]. For the numerical approximation of warpage, structural load cases were applied on the geometry after the "Fill + Pack" analysis was completed.

Experimental validation of simulation results that focused on fibre orientation and part warpage was performed on a single cavity prototype mould (the full design layout being proprietary) with the PP 30% fibre-filled grade. Further details of the experimental work will be discussed in Section 3.3.

3. Results and discussion

To ensure that computational instabilities due to mesh were attenuated, a mesh convergence study was conducted to select the most suitable mesh to be employed in present study. The following sections, in subsequent order, present the results of the analyses.

3.1. The effect of gate location and material selection on warpage

As a function of materials and gate locations, the computed warpage (deflection) after the analysis cycle is presented in Fig. 3. The analysis considered the material properties summarised in Table 1, and the warpage due to the total variation in shrinkage and fibre orientation (only for the PP 30% grade) was computed.

The all deflection result is represented by the sum of deflections in the XYZ directions. The average all deflections were found to be 0.45, 0.25 and 0.33 mm for the PP, PS and PP 30% fibre-filled grade respectively. It was presumed that the part would warp towards the gate locations, hence the Z-direction deflection was also plotted. This assumption proved to be correct as the average Z-direction deflection contributed, in this order: 55%, 49%, and 62% to the all deflection in relation to PP, PS, and PP 30% fibre-filled grades. The greatest all (and Z-direction) deflection values were observed with the PP for each gate location. This magnitude of deflection can be attributed to the crystalline nature, high thermal expansion and low elastic and shear moduli of this grade (Table 1). The PS could effectively be used to reduce the warpage by as much as ~50% compared to the PP. As being an amorphous grade, the variation of shrinkage and thermal expansion are smaller, whereas it has higher elastic and shear moduli (Table 1) representing a greater resistance against deflection compared to PP.

However, no clear tendency for the PP and PS can be observed in terms of improving the warpage with different gate locations. At this point, it may be stated that the PS would be the best choice based on warpage characteristics compared to PP.

On average, the PP 30% fibre-filled grade (also being a crystalline material) showed greater deflection in contrast to the PS, although less than the PP. If that was used, the effect of gate location would become more conspicuous. This suggests that the warpage characteristic shows fibre orientation dependent behaviour. This effect will be discussed in detail in Section 3.3.

However, it should be highlighted that the lowest thermal expansion and highest elastic and shear moduli are associated with the PP 30%, therefore the minimised warpage and maximised structural stiffness can only be achieved using this grade with the gate positioned at the top of the part.

3.2. The evaluation of injection pressure and cavity fill patterns

To be able to improve the moulding process, the investigation is extended with respect to the assessment of melt flow characteristics. For this, the viscosity of the materials was also used as a reference material property (Table 1) which was correlated with the numerically predicted injection pressure. As a function of materials and gate locations, the data are plotted in Fig. 4.

As a function of PP, PS and PP 30% fibre-filled materials, the injection pressure in this order, decreased with the snap, bottom, middle and top gate locations. This is in direct correlation with the viscosity of the melt and it may be stated that the lower the viscosity, the lower the

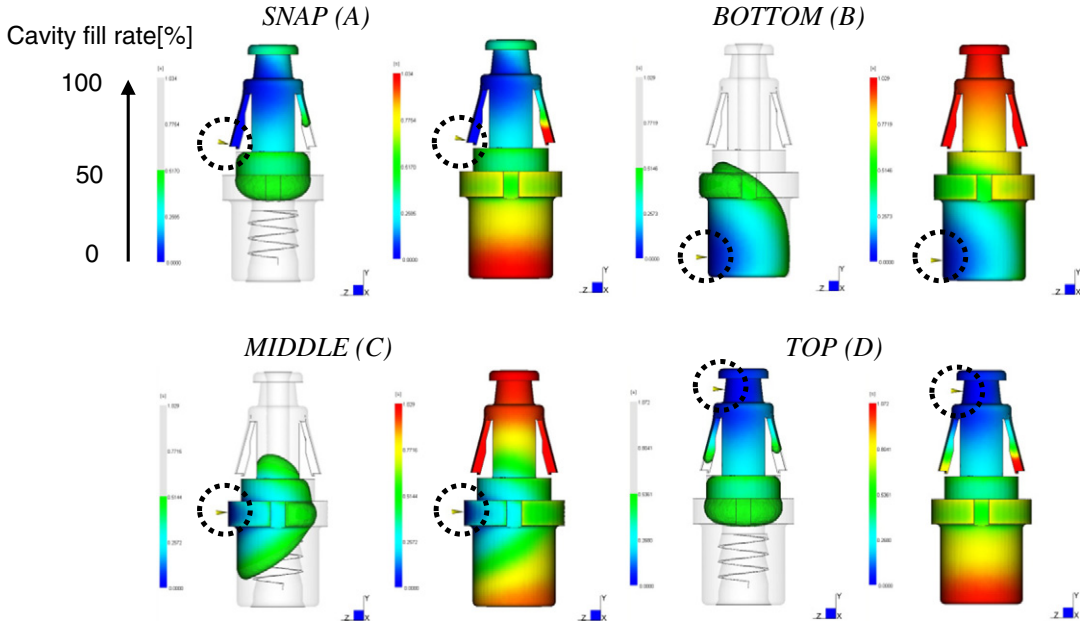

Fig. 6. Melt front evolution as a function of gate locations for the PP 30% fibre-filled grade.

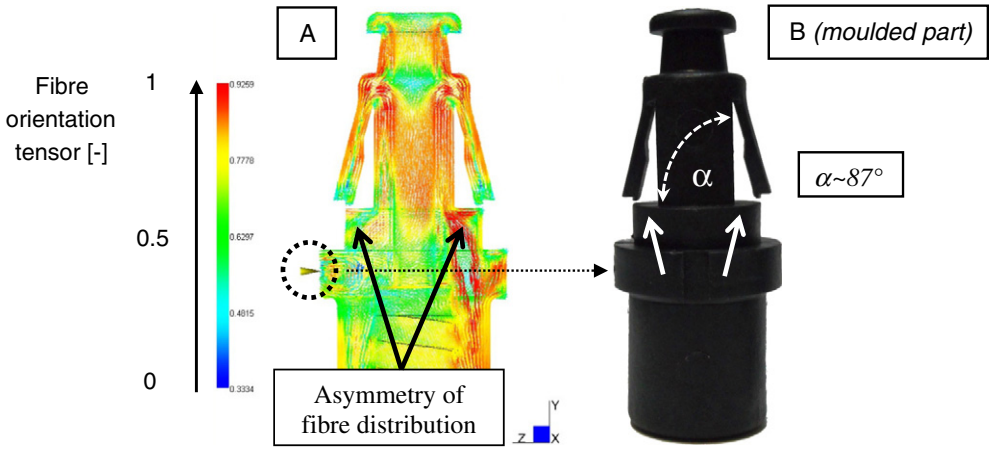

Fig. 7. Fibre orientation and real part deflection with the middle gate.

resistance of the melt to flow, therefore less injection pressure is needed to fill the cavity.

Without discussing the effects of additional material properties such as thermal conductivity and specific heat capacity, Eq. (17) can be used to relate the change in heat energy (i.e. the change in viscosity) as a function of time. It expresses that the (average) heat flow is proportional to the area and the temperature difference, but inversely proportional to the cross-section [5].

$$\frac{\Delta Q}{\Delta t} \sim A\frac{\Delta T}{\Delta x} \tag{17}$$

where, $\Delta Q/\Delta t$ is the heat flow (across the melt), A is the surface cross-sectional area and $\Delta T/\Delta x$ is the change in (melt) temperature with cross-section x.

The effect of melt viscosity together with variations in cross-section is most easily recognisable if the gate was positioned at the snap feature of the part. Since the cross-sectional area of the snap is ~50 mm^2 and the local thickness for flow is minimal ~1.5 mm, the heat from the melt is quickly lost by conduction into the mould. A more rapid fall in melt temperature facilitates the formation of the frozen layer and gives a rise in viscosity which in turn, increases the injection pressure.

For instance, the results of computed injection pressure suggest that the highest injection pressure with the snap gate location were 7, 6, and 2.4 MPa for the PP, PS, and PP 30% fibre-filled grade respectively. With the bottom and middle gate locations, where the local thicknesses are ~3 and ~5 mm, similar pressure values were predicted compared to each other. As an indication these were ~4.5/3.9, ~4.1/3.6 and ~1.5/1.4 MPa. However, if top gate location was applied, with the local thickness of ~2 mm, the lowest pressures ~2.5, ~2 and ~0.8 MPa would be estimated.

By taking into consideration that the maximum material stiffness and a compromise between reduced warpage and injection pressure was associated with the PP 30% fibre-filled grade, this was chosen for further analysis.

At this stage it is worth to point out that not only is it important to know the injection pressure, but also the pressure loss due to the melt flow. The gate should be positioned in a way that the mould fills uniformly and the associated pressure drop is minimal. The loss in injection pressure during cavity filling can have detrimental consequences, such as melt flow hesitation or air entrapment [22]. Therefore, it is desirable to consider this parameter as well in order to achieve improved part quality.

In Fig. 5, as a function of gate locations the injection pressure loss (the difference of maximum and minimum injection pressure occurring due to variations in pressure from region to region of the part) is plotted. As a reminder, the injection pressure is also added to the graph. As an indication, if the snap gate location is used, the molten material that enters the thin snap feature slows down and loses heat resulting in increased viscosity, high injection pressure and pressure loss. The greatest pressure drop was predicted with the snap gate location, followed by the top, bottom and middle gate positions. However, the best and second best options between reduced injection pressure and pressure loss are represented by the top and middle gate locations.

To better understand how the melt flows in the cavity, the flow patterns of the PP 30% fibre-filled grade are depicted in Fig. 6 (with injection locations marked by dotted circles). For each gate location, two images are rendered. The left ones illustrate the flow at ~50% fill

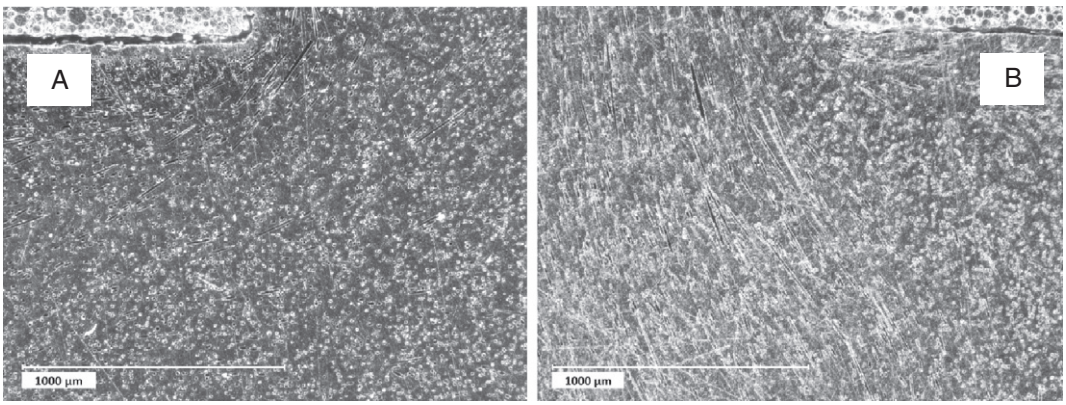

Fig. 8. The asymmetry of fibre distribution with the middle gate, towards the gate side (A) and opposite to gate side (B).

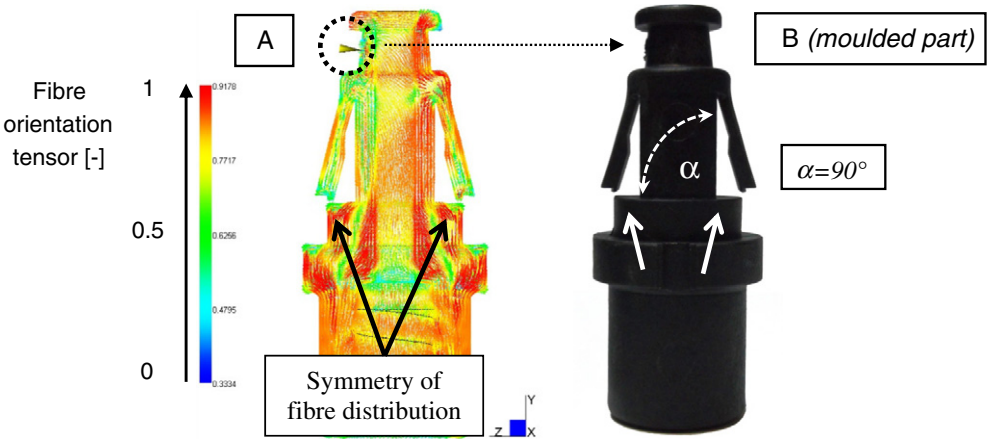

Fig. 9. Fibre orientation and real part deflection with top gate.

rate, while the full contours represent the final flow patterns right after cavity filling.

The gate positioned at the snap creates a flow problem called hesitation (Fig. 6(A)). This is best seen as the melt front at the right-hand side snap slows down in contrast to the mainstream flow that advances towards the bottom of the part. Also, it can be noticed that the flow advancement with the bottom and middle gate locations are not uniform either (Fig. 6(B, C)). This is most easily recognisable at ~50% fill and is due to the variation in cross-section as well as flow length. Moreover, a bidirectional flow pattern was observed with the middle gate location (Fig. 6(C)).

To overcome this difficulty, the top gate location provides the best alternative. With this option, both the snap features and the bottom of the part would fill nearly at the same time. Some flow hesitation does exist, however not as severe as with the snap gate location. The hesitation effect with the top gate location is offset by having the most unidirectional flow pattern generated (Fig. 6(D)). The aforementioned bidirectional and unidirectional flow patterns have dominant influence on fibre orientation and therefore on part warpage that will be discussed in Section 3.3.

3.3. Numerical prediction for fibre orientation and experimental validation

In order to discover the effect of fibre orientation on part warpage, simulations and injection moulding trials were conducted using the PP 30% fibre-filled grade. This part of the work utilised the top and middle gate locations for both computational and experimental analysis. According to Fig. 5, these two gate locations represented the best and second best alternatives in terms of minimum injection pressure (and pressure loss). In addition, as mentioned earlier, the middle gate location permitted to study the effect of bidirectional melt flow evolution.

For the moulding trials the following process settings were applied (identical to the computational conditions): 240/40 °C melt/mould temperatures, 1 s injection time, packing pressure maintained at 80% of filling pressure for 5 s, with cycle time being ~30 s.

With respect to numerically obtained fibre orientation and experimentally observed part warpage, the major differences between these gate options are explained below.

In Fig. 7(A) the red areas of the fibre orientation contour plot indicate high probability (~1) of fibre alignment and blue areas refer to lower probability (~0) respectively [26]. The results for computed fibre orientation on the cross-sectioned part (YZ plane) suggests, that as in the case of middle gate, the fibres tend to align horizontally in the X direction near the gate, while there is vertical alignment at the opposing side of part in the Y direction. As a result, the asymmetrical distribution of fibres causes the part to warp towards the gate (Z direction) where unrestricted shrinkage exists. In Fig. 7(B) the injection moulded sample clearly confirmed this effect. By using image analysis techniques, the angle of deformation was found to be α ~ 87°, in contrast to the computed ~89°.

Light microscope images also revealed the asymmetry of fibre distribution. The images were taken on the cross-sectioned part at the areas highlighted with white arrows in Fig. 7(B). Fig. 8(A) shows the fibre alignment in the X direction near the gate (fibres are seen as dots) while Fig. 8(B) illustrates fibre alignment in the Y direction respectively.

The angle (or magnitude) of deformation can be a critical parameter for several engineering applications. For instance, plastic covers and

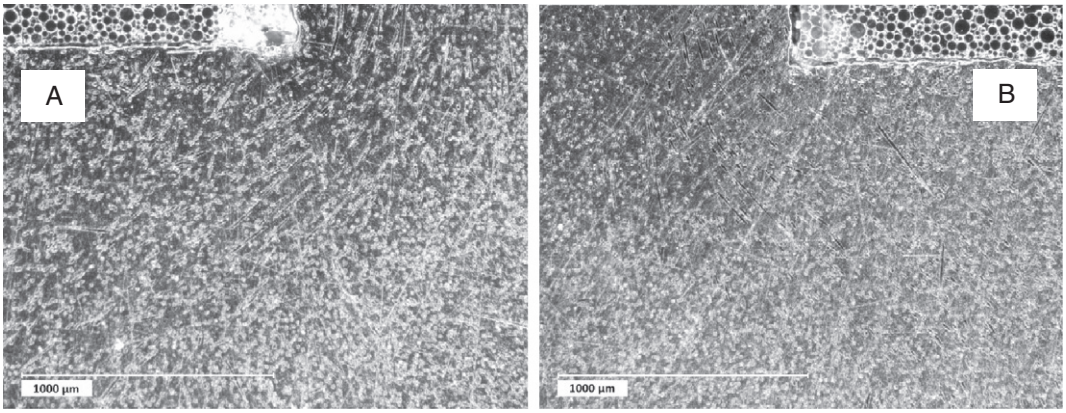

Fig. 10. The symmetry of fibre distribution with the top gate, towards the gate side (A) and opposite to gate side (B).

housings can be joined together to form more complex assemblies. Even the smallest part misalignment may cause incomplete/loose fitness or compromise the load-bearing capacity, resulting in premature component failure. Therefore the elimination of this problem is critical and the potential solution is presented below.

By applying the top gate location, the melt will flow from the top section towards the bottom of the part, generating a more uniform fibre orientation pattern, as illustrated in Fig. 9(A). Differential orientation was still predicted near the gate, however the orientation being symmetrical at the critical mid-section of the part, ensuring improved warpage. In this case, the computed and measured angle of was found to be $\alpha = 90°$, representing the ideally straight alignment of the part, as depicted in Fig. 9(B).

Fig. 10(A) and (B) depicts that symmetrical fibre distribution exists with the top gate location. The images were taken on the cross-sectioned part (YZ plane) at the areas highlighted with white arrows in Fig. 9(B).

4. Conclusions

The effects of materials selection and gate location with respect to reduction in warpage and injection pressure were presented. The analysis utilised a case study that demonstrated a step-by-step methodology to discover the complex relationship between the parameters mentioned above. The numerical analysis used a commercial flow package that investigated the warpage characteristics and injection pressure values of three thermoplastic grades along with four injection locations.

Due to variations in shrinkage characteristics the warpage results showed dependency on grade types. The effect of gate locations was the most noticeable with the fibre-filled PP. In an attempt to maximise the mechanical performance of the component, higher part stiffness may be achieved by selecting the fibre-filled PP for injection moulding.

Further to this, the lowest injection pressure was associated with the fibre-filled PP. By utilising this grade for further analysis, it became clear that reduced injection pressure (and also pressure loss) were associated with the middle and top gate locations.

With respect to fibre alignment, an asymmetrical fibre distribution would be generated if the middle gate location was applied. Contrary to this, symmetrical fibre distribution could be achieved with the top gate location. The tendency for warpage was observed by numerical analysis and showed excellent agreement with experimental validation. With the middle gate location the angle of deformation was estimated to be $\alpha \sim 87°$, while elimination of warpage was achieved with the top gate location with deformation angle being $\alpha = 90°$. Therefore, differential fibre orientation did not cause warpage, but the asymmetrical distribution of fibre orientation did.

The important finding is that the final gate location should only be chosen after the relevant material properties (e.g. shrinkage characteristics, mechanical properties and viscosity) and melt flow direction have been taken into account. The successful elimination of warpage and reduction in injection pressure and can give multiple benefits. With the careful selection of materials and gate location, not only can the mould design be optimised but the production waste and energy costs minimised as well, making a step towards sustainable manufacturing.

Acknowledgements

The authors would like to acknowledge the support of the Advanced Sustainable Manufacturing Technologies (ASTUTE) project, which was part funded from the EU's European Regional Development Fund through the Welsh European Funding Office.

References

[1] H. Zhou, Computer modeling for injection molding: simulation, optimization and control, John Wiley & Sons Inc., 2013. (ISBN 978-0-470-60299-7).
[2] G. Potsch, W. Michaeli, Injection molding, an introduction, munich: carl hanser verlag(ISBN-13: 978-1-56990-419-0) 2008.
[3] T.A. Osswald, L.-S. Turng, P. Gramman, Injection molding handbook, Carl Hanser Verlag, Munich, 2008.
[4] H. Hassan, N. Regnier, C. Le Bot, G. Defaye, 3D study of cooling system effect on the heat transfer during polymer injection molding, Int. J. Therm. Sci. 49 (2010) 161–169.
[5] P. Kennedy, R. Zheng, Flow analysis of injection molds, 2nd ed. Carl Hanser Verlag, Munich, 2013. (ISBN 978-1-56990-512-8).
[6] S.-W. Kim, L.-S. Turng, Three-dimensional numerical simulation of injection molding filling of optical lens and multiscale geometry using finite element method, Polym. Eng. Sci. 46 (2006) 1263–1274.
[7] L. Seow, Y. Lam, Optimizing flow in plastic injection molding, J. Mater. Process. Technol. 72 (1997) 333–341.
[8] H. Hassan, N. Regnier, G. Defaye, A 3D study on the effect of gate location on the cooling of polymer by injection molding, Int. J. Heat Fluid Flow 30 (2009) 1218–1229.
[9] J. Shoemaker, Moldflow design guide, Carl Hanser Verlag, Munich, 2006. (ISBN-13: 978-1-56990-403-9).
[10] K.-M. Tsai, C.-Y. Hsieh, W.-C. Lo, A study of the effects of process parameters for injection molding on surface quality of optical lenses, J. Mater. Process. Technol. 209 (2009) 3469–3477.
[11] M. Song, Z. Liu, M. Wang, T. Yu, D. Zhao, Research on effects of injection process parameters on the molding process for ultra-thin wall plastic parts, J. Mater. Process. Technol. 187-188 (2007) 668–671.
[12] B. Ozcelik, I. Sonat, Warpage and structural analysis of thin shell plastic in the plastic injection molding, Mater. Des. 30 (2009) 367–375.
[13] S. Tang, Y. Tan, S. Sapuan, S. Sulaiman, N. Ismail, R. Samin, The use of Taguchi method in the design of plastic injection mould for reducing warpage, J. Mater. Process. Technol. 182 (2007) 418–426.
[14] N. Subramanian, T. Lin, Y.A. Seng, Optimizing warpage analysis for an optical housing, Mechatronics 15 (2005) 111–127.
[15] B. Mlekusch, The warpage of corners in the injection moulding of short-fibre-reinforced thermoplastics, Compos. Sci. Technol. 59 (1999) 1923–1931.
[16] E. Bociaga, T. Jaruga, K. Lubczynska, A. Gnatowski, Warpage of injection moulded parts as the result of mould temperature difference, Arch. Mater. Sci. Eng. 44 (1) (2010) 28–34.
[17] R. Sánchez, J. Aisa, A. Martinez, D. Mercado, On the relationship between cooling setup and warpage in injection molding, Measurement 45 (2012) 1051–1056.
[18] Y.-H. Lin, H.-L. Chen, S.-C. Chen, Y.-C. Lin, Effect of asymmetric cooling system on in-mold roller injection molded part warpage, Int. Commun. Heat Mass Transfer 61 (2015) 111–117.
[19] A.W. Birley, B. Haworth, J. Batchelor, Physics of plastics: processing, properties and materials engineering, Carl Hanser Verlag, Munchen, 1991. (ISBN 3-446-16274-7).
[20] T.A. Osswald, G. Menges, Materials science of polymers for engineers, Carl Hanser Verlag, Munchen, 1996. (ISBN 1-56990-192-9).
[21] M.A. Rosen, H.A. Kishawy, Sustainable manufacturing and design: concepts, practices and needs, Sustainability 4 (2004) 154–174.
[22] R.A. Malloy, Plastic part design for injection molding, an introduction, 2nd ed. Carl Hanser Verlag, Munnich, 2010. (ISBN-13: 978-1-56990-7).
[23] Y.K. Shen, W.Y. Wu, An analysis of three-dimensional micro-injection molding, Int. Comm. Heat Mass Transfer 29 (3) (2002) 423–431.
[24] W.-H. Yang, A. Peng, L. Liu, D.C. Hsu, Integrated numerical simulation of injection molding using true 3D approach, SPE ANTEC, USA, 2004.
[25] Y.-K. Shen, C.-W. Wu, Y.-F. Yu, H.-W. Chung, Analysis for optimal gate design of thin-walled injection molding, Int. Commun. Heat Mass Transfer 35 (2008) 728–734.
[26] Autodesk Inc., Simulation Moldflow Insight, 2014.
[27] N.M. Neves, A.J. Pontes, A.S. Pouzada, Effect of the interaction coefficient in the prediction of the fiber orientation of injection molded glass fiber reinforced polycarbonate, SPE ANTEC, Portugal, 2000.